Oscillatory Magnetoresistance in Mercuric Selenide

CHARLES R. WHITSETT*
Union Carbide Research Institute, Tarrytown, New York
(Received 8 December 1964)

The oscillatory magnetoresistance (Shubnikov–de Haas effect) in oriented single crystals of mercuric selenide was measured at 1.2 and 4.2°K and in transverse magnetic fields up to 25 kG. Analysis of the periods of the oscillations for the magnetic field aligned with ⟨110⟩, ⟨111⟩, and ⟨100⟩ crystallographic directions showed that the Fermi surface for conduction electrons in HgSe, although nearly spherical, has slight bulges in the ⟨111⟩ directions of **k** space. From the temperature dependence of the amplitudes of the oscillations, it was determined that the cyclotron effective masses of conduction electrons at the Fermi surface ranged from 0.033 to 0.068 m_e for samples having from 1.86×10^{17} to 4.52×10^{18} electrons/cm³. This variation of effective mass with electron concentration is consistent with the nonparabolic conduction-band model developed for compounds that have the zincblende crystal structure. The band parameters derived are $p=7.1\times10^{-8}$ eV cm and $E_G=0.24$ eV, where P is an interband momentum matrix element and E_G is the band gap at $\mathbf{k}=0$; these values are in fair agreement with parameters deduced from reflectivity data by other investigators.

INTRODUCTION

MERCURIC selenide (HgSe) has a unique combination of properties which make it one of the classic materials for detailed investigations of solid-state phenomena. It has the same cubic-zincblende crystal structure as the semiconducting III–V compounds, and the growth of single crystals and the zone refining of HgSe are not difficult. The compound is classified by its electrical properties[1–3] as a semimetal or degenerate semiconductor, and it is characterized by a large electron mobility (as high as 18 500 cm²/V sec at 300°K). The lattice thermal conductivity above 100°K is unusually low, and this together with the favorable electrical characteristics is responsible for large magnetothermal effects[4,5] in HgSe. Among the phenomena which have been investigated in HgSe are the Nernst-Ettingshausen effect,[6] the thermoelectric power,[1,7] the Corbino magneto-Seebeck effect,[8] photoelectron emission,[9] the photovoltaic effect,[1] and optical absorption and reflectivity.[1,2,10–12]

The conduction band in HgSe is nearly spherically symmetric, but nonparabolic, as evidenced by the angular dependence of magnetoresistance[1,13] and by reflectivity[11] data. This is confirmed by the results to be presented here of measurements of the oscillatory magnetoresistance (Shubnikov–de Haas effect) of HgSe at 1.2 and 4.2°K. Measurements were made on oriented single crystals which had conduction-electron densities that ranged from 2×10^{17} to 4.5×10^{18} electrons/cm³. Cyclotron effective masses are deduced here from the temperature dependence of the amplitudes of the oscillations, and the observed dependence of effective mass upon electron concentration may be explained by a nonparabolic conduction-band model similar to that developed for InSb. From the nature of the variation of oscillatory magnetoresistance with changing magnetic-field direction, it is concluded that the Fermi surface, although nearly spherical, has slight bulges along ⟨111⟩ directions in **k** space.

The band model for HgSe in Fig. 1 is based on results by Harman and Strauss[2] who found it necessary to assume the 0.07-eV overlap of the conduction and valence bands in order to account satisfactorily for the temperature dependence of the Hall effect. Their data showing the optical-absorption-edge energy to be strongly dependent upon the conduction electron density and to be always less than the Fermi energy are consistent with the hypothesis of the band overlap. Wright, Strauss, and Harman[11] determined from reflectivity data the dependence at room temperature of cyclotron effective mass upon electron concentration and found that this dependence is satisfactorily accounted for by the nonparabolic conduction band model derived by Kane[14] for InSb. Their analysis of the effective-mass variation based upon Kane's equations yielded the value of 0.2 eV for the energy gap at the origin of **k** space. Using this model, Harman[15] has been able to account in detail for the many experimental observations of electron-transport phenomena in HgSe.

The forms of the valence bands as shown in Fig. 1 are

* Present address: Research Division, McDonnell Aircraft Corporation, St. Louis, Missouri.

[1] H. Gobrecht, U. Gerhardt, B. Peinemann, and A. Tausend, J. Appl. Phys. **32**, 2246 (1961).
[2] T. C. Harman and A. J. Strauss, J. Appl. Phys. **32**, 2265 (1961).
[3] M. D. Blue and P. W. Kruse, J. Phys. Chem. Solids **23**, 577 (1963).
[4] Kh. I. Amirkhanov, A. Z. Daibov, and V. P. Zhuze, Dokl. Akad. Nauk SSSR **98**, 557 (1954).
[5] C. R. Whitsett, J. Appl. Phys. **32**, 2257 (1961).
[6] I. M. Tsidil'kovskii, Zh. Techn. Fiz. **27**, 12 (1957) [English transl.: Soviet Phys.—Tech. Phys. **2**, 9 (1957)].
[7] M. Rodot and H. Rodot, Compt. Rend. **250**, 1447 (1960).
[8] T. C. Harman, Phys. Rev. **118**, 1541 (1960).
[9] O. M. Sorokin, Zh. Techn. Fiz. **28**, 1413 (1958) [English transl.: Soviet Phys.—Tech. Phys. **3**, 1311 (1958)].
[10] D. Redfield, Bull. Am. Phys. Soc. **2**, 121 (1957).
[11] G. B. Wright, A. J. Strauss, and T. C. Harman, Phys. Rev. **125**, 1534 (1962).
[12] M. Cardona and G. Harbeke, J. Appl. Phys. **34**, 813 (1963).
[13] T. C. Harman, J. Appl. Phys. **32**, 1800 (1961).
[14] E. O. Kane, J. Phys. Chem. Solids **1**, 249 (1957).
[15] T. C. Harman, J. Phys. Chem. Solids **25**, 931 (1964).

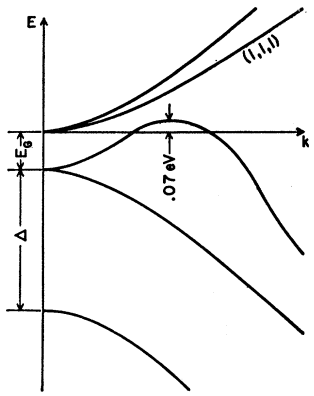

FIG. 1. Proposed band structure for HgSe. Value of 0.07 eV for band overlap is from Ref. 2; qualitative shape of heavy-hole valence band after Ref. 16. Depiction of ⟨111⟩ conduction band as lowest lying is based upon results in this paper.

based qualitatively upon results by Cardona[16] who extended Kane's method to calculate band parameters for a number of semiconductors that have the diamond, zincblende, or wurtzite crystal structures. The depiction in Fig. 1 of the conduction band along the [111] direction as that having relatively the least curvature near the origin is based upon the conclusions of the present paper. [*Note added in proof.* T. C. Harman has pointed out to the author that an overlap of the Γ_{15} valence band with the conduction band, as shown in Fig. 1, would imply a larger pressure coefficient of resistivity than 1%/kbar which actually is observed.[16a] The origin and nature of the overlapping valence band is not known.]

Measurements of the Shubnikov–de Haas effect contribute to the understanding of the nature of HgSe, but also they are of interest in themselves because of the opportunity they afford for testing the theories of electron-quantum-transport phenomena and for acquiring new insight into the details of such phenomena. It will be shown that present theories do satisfactorily describe many of the observations of HgSe. Since mercuric selenide has one of the simplest band structures of any material for which the oscillations of magnetoresistance are easy to measure, this compound should be valuable for studying electron processes in the quantum limit at high magnetic fields and for studying other phenomena, such as electronic specific heat and the thermoelectric power, which may exhibit oscillatory behavior.

THE SHUBNIKOV–DE HAAS EFFECT

Oscillations in electrical resistivity as a function of magnetic field were first observed, in bismuth, by Shubnikov and de Haas.[17] In recent years studies of oscillatory magnetoresistance and oscillatory magnetic susceptibility (de Haas–van Alphen effect) in metals and semiconductors have provided a detailed knowledge of the electron energy band structures in these materials. The theories of magnetoresistance oscillations and many experimental results have been reviewed by Kahn and Frederikse.[18]

In the absence of a magnetic field a free-electron system may be treated as having a nearly continuous and even distribution of quantum states in momentum space. Under the influence of a magnetic field these states are condensed into a set of cylindrical Landau surfaces parallel to the magnetic-field direction and with cross-sectional areas normal to the field direction given by

$$A_N=(N+\tfrac{1}{2})(2\pi eB/\hbar c), \tag{1}$$

where N is an integer or zero and B is the magnetic induction. The allowed energies are

$$E_N=(N+\tfrac{1}{2})\hbar\omega+\hbar^2k_z^2/2m_e \tag{2}$$

if B is in the z direction, ω is the cyclotron frequency eB/cm_e, and m_e is the free electron mass. As the magnetic-field intensity increases the Landau cylinders expand and one by one are excluded from the volume enclosed by the Fermi energy surface. If the energy separation $\hbar\omega$ of the cylinders is larger than kT (k=Boltzmann constant) but smaller than E_F, the zero-field Fermi energy, then the passing of the cylinders through the Fermi surface will result in observable periodic changes in the electronic properties of the system. A further requirement for the magnetic quantization to produce observable effects is that the mean time τ between electron-scattering events be large compared with the cyclotron period $1/\omega$. Thus, for oscillatory phenomena there are in general three conditions that must be satisfied: $\hbar\omega<E_F$, $\hbar\omega>kT$, and $\omega\tau>1$.

The oscillations for a free electron system will be periodic in $1/B$ with the period

$$P_F=\hbar\omega/BE_F=2\pi e/\hbar cA_F, \tag{3}$$

where A_F is the maximum cross-sectional area of the Fermi surface normal to the magnetic-field direction. For free electrons the period depends only upon the electron density n:

$$P_F=(2e/\hbar c)(3\pi^2n)^{-2/3}=3.18\times10^6n^{-2/3}, \tag{4}$$

where the numerical factor is that appropriate to give P_F in units of gauss^{-1} if n is expressed in cm^{-3}.

A result derived by Adams and Holstein[19] in their treatment of quantum transport effects in a free electron system, and which will serve as a basis for analysis in this paper, is the following expression for one component

[16] M. Cardona, J. Phys. Chem. Solids **24**, 1543 (1963).
[16a] J. A. Kafalas, H. C. Gatos, M. C. Lavine, and M. D. Banus, J. Phys. Chem. Solids **23**, 1541 (1962).
[17] L. Shubnikov and W. J. de Haas, Leiden Comm. **207a** and **207d** (1930).
[18] A. H. Kahn and H. P. R. Frederikse, in *Solid State Physics*, edited by F. Seitz and D. Turnbull (Academic Press Inc., New York, 1959), Vol. 9, p. 257.
[19] E. N. Adams and T. D. Holstein, J. Phys. Chem. Solids **10**, 254 (1959).

of the oscillatory magnetoconductivity:

$$\frac{\Delta\sigma_1}{\sigma_0}=5\left(\frac{\pi\hbar\omega}{E_F}\right)^{1/2}\sum_{M=1}^{\infty}\frac{(-1)^M\exp(-2\pi M\gamma)}{(2\pi M)^{1/2}}\times\left(\frac{M\xi}{\sinh M\xi}\right)\cos\left(\frac{2\pi ME_F}{\hbar\omega}-\frac{\pi}{4}\right), \quad (5)$$

where $\xi=2\pi^2kT/\hbar\omega$, σ_0 is the zero-field conductivity, and γ is a nonthermal damping factor which is dependent upon the nature of the electron-scattering mechanism and which also is influenced by nonhomogeneity of the system. For a homogeneous system γ should be of the order of $1/\mu_0B$ where μ_0 is the zero-field electron mobility. Equation (5) is valid when the oscillations are small compared with the nonoscillatory part of the magnetoconductivity, and when E_F is much larger than $\hbar\omega$. Usually, only the first harmonic ($M=1$) is observed experimentally, and the oscillations appear to be exponentially damped cosine functions.

The free electron results given so far will also be valid for systems for which the zero field electron energy E_0 is a function only of the magnitude of $\mathbf{k}$, provided that for m_e is substituted the cyclotron effective mass m_H, given by

$$m_H=\hbar^2k(dE_0/dk)^{-1}. \quad (6)$$

If E_0 is a more complicated function of $\mathbf{k}$, then the result of Lifshits and Kosevich[20] must be employed. That is, for an arbitrary Fermi surface geometry the period of the resistance oscillations is given by

$$P=2\pi e/\hbar cA, \quad (7)$$

where A is the maximum or minimum cross-sectional area of the Fermi surface normal to the magnetic-field direction.

For Fermi surfaces which have more than one extremal cross-sectional area normal to a given magnetic-field direction, there will be oscillatory effects associated with each such area. If the areas are significantly different the periods associated with each of the areas are often easy to deduce from the experimental data; otherwise, they produce "beat" effects. Such beat patterns may be quite complicated because the amplitudes of the oscillations arising from the various extremal areas may be different and have different field dependences.

EXPERIMENTAL PROCEDURE

Oriented single crystals of HgSe, about $1\times1\times10$ mm^3 in size, were used for the resistance measurements. The long dimension of each crystal was in a ⟨110⟩ direction, and the sides were {110} and {100} planes. The samples were suspended vertically in a horizontal magnetic field. By rotating a sample about its vertical ⟨110⟩ axis, sets of {100}, {111}, and {110} planes in turn could be aligned normal to the magnetic-field direction.

After a sample was cut and lapped to size it was etched for 1–2 sec in bromine and then rinsed in a solution of ethyl alcohol and benzene to remove selenide residues in accordance with a technique described by Harman.[13] The sample was then annealed at approximately 200°C either in vacuum or mercury vapor to so alter the excess of mercury over stoichiometry to achieve a desired conduction electron concentration in the range of from less than 2×10^{17} to 4.5×10^{18} electrons/cm^3 at 4.2°K.

Current leads were joined to the ends of a sample with silver paint. Hall and resistivity probes were 0.002-in.-diam platinum wires which were spark welded to the crystal sides. The platinum probes were so mounted that they would remain in place and in contact with the crystal even if a weld joint should fail because of thermal shock. Thus, when a weld failure did occur during cooling of the sample by liquid helium, the weld could be re-established without removing the sample from the liquid-helium bath.

Currents of from 50 to 150 mA from a battery source were passed through the samples for resistivity measurements. The voltage between the resistance probes was amplified and then applied to the Y input of an X-Y recorder. An ac signal proportional to magnetic field intensity was supplied by a rotating coil fluxmeter probe and, after conversion to a proportional dc voltage, was applied to the X input of the X-Y recorder. At a given temperature the magnetic field was slowly varied between 5 and 25 kG, and a plot of resistance voltage versus magnetic field was traced by the X-Y recorder. The resistance voltage was sufficiently amplified and then bucked by a dc voltage so that the oscillatory component alone would be as large in amplitude as possible on the X-Y record.

Envelopes of the oscillatory resistance voltage maxima and minima were drawn on the X-Y record. The curve midway between the upper and lower envelopes was used as the base line for measuring the amplitudes of the oscillations.

RESULTS

The oscillatory component of magnetoresistance $\Delta\rho/\rho_0$ is plotted for a series of samples having successively higher electron concentrations in Figs. 2–6. The oscillatory component $\Delta\rho$ was computed by subtracting from the total resistivity the average of the upper and lower envelopes of the resistivity oscillations; ρ_0 is the zero-field resistivity. In Figs. 2–6 curves are shown for the magnetic field aligned with ⟨110⟩, ⟨111⟩, and ⟨100⟩ crystallographic directions. The solid curves were obtained with the samples at approximately 4.2°K; the dotted curves (or dotted envelopes of the oscillations in Figs. 5 and 6) were obtained at approximately 1.2°K.

[20] E. M. Lifshits and A. M. Kosevich, J. Phys. Chem. Solids 4, 1 (1958).

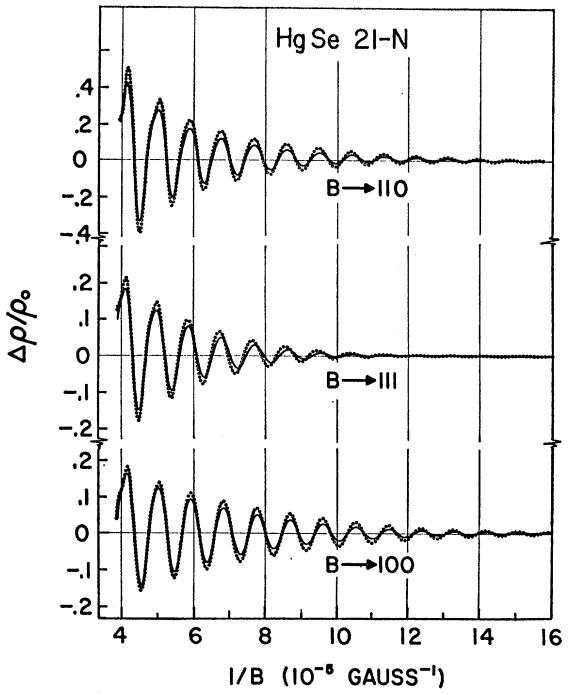

FIG. 2. Oscillatory component of magnetoresistance of HgSe-N; solid curves for 4.2°K, dotted curves for 1.2°K. At 4.2°K, $n=2.08\times10^{17}$ electrons/cm³ and $\mu_0=156\,000$ cm²/V sec. Periods differ slightly for different magnetic-field directions, but only one frequency component is observed for a given magnetic-field alignment.

The periods and amplitudes of the oscillations decrease as the electron concentrations of the samples increase. In most cases the periods for 1.2°K are slightly smaller than those for 4.2°K. As the electron concentration increases a beating in the oscillations is strong for the magnetic field in the ⟨111⟩ and ⟨100⟩ directions. However, no beating ever occurs for the magnetic field in a ⟨110⟩ direction. As the samples were rotated so that in turn the ⟨110⟩, ⟨111⟩, and ⟨001⟩ directions were aligned with the magnetic-field direction, the ⟨110⟩ pattern gradually was altered with the beat pattern intensifying until the ⟨111⟩ beat pattern was obtained; then the ⟨111⟩ beat pattern would disappear and the ⟨001⟩ beat pattern would gradually build up.

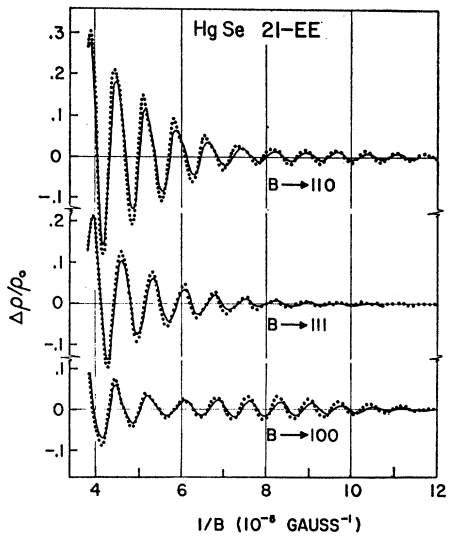

FIG. 3. Oscillatory component of magnetoresistance of HgSe-EE; solid curves for 4.2°K, dotted curves for 1.2°K. At 4.2°K, $n=3.47\times10^{17}$ electrons/cm³ and $\mu_0=90\,900$ cm²/V sec. Lowest electron concentration for which beating was observed.

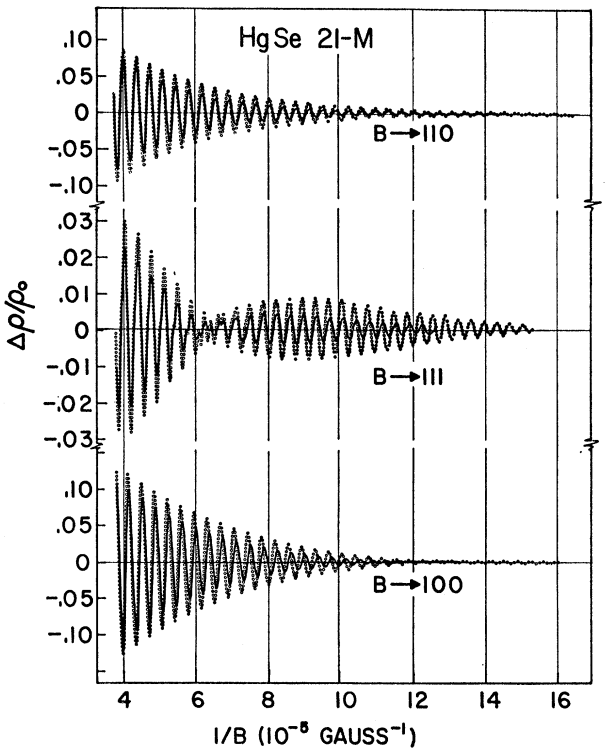

FIG. 4. Oscillatory component of magnetoresistance of HgSe-M; solid curves for 4.2°K, dotted curves for 1.2°K. At 4.2°K, $n=8.46\times10^{17}$ electrons/cm³ and $\mu_0=49\,200$ cm²/V sec. Beating was evident for B in ⟨100⟩ directions as well as ⟨111⟩ directions, but is not apparent after reduction of drawing.

The amplitudes usually were smaller, and decayed more rapidly as B decreased, for the magnetic field in a ⟨111⟩ direction. Also, for many of the samples the nonoscillatory component varied widely and was undoubtedly due largely to the inhomogeneity of the material in the vicinity of the probe welds. Different behavior was observed at times when the probes were replaced on the same sample. The behavior of the nonoscillatory part of the resistance did not affect the periods or forms of the oscillations, but it did occasionally slightly affect the amplitudes. Since for some samples the nonoscillatory magnetoresistance was small and increased very slowly with field, it is likely that in really homogeneous material the steady magnetoresistance is small compared with the oscillatory component.

The ⟨110⟩ oscillations in every case have only one

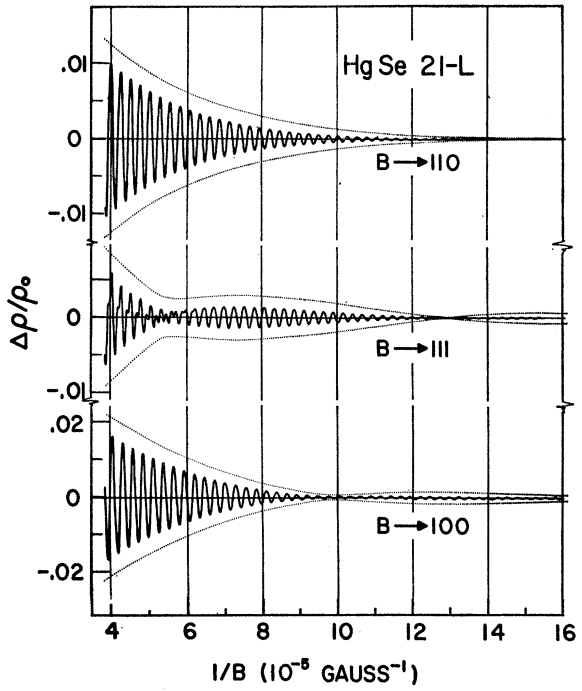

FIG. 5. Oscillatory component of magnetoresistance of HgSe-L; solid curves for 4.2°K, dotted curves for envelopes of oscillations at 1.2°K. At 4.2°K, $n=1.34\times10^{18}$ electrons/cm³ and $\mu_0=80\,200$ cm²/V sec. Complete beat period is observed for B in ⟨111⟩ directions.

frequency component. The ⟨111⟩ and ⟨100⟩ oscillations for all samples except those with the lowest electron concentrations are superpositions of two oscillations that have nearly the same frequencies. Thus, in the ⟨111⟩ and ⟨100⟩ cases, the oscillations have a short period and a long period corresponding to sum and difference beat frequencies. Figure 7 shows X-Y recorder traces of resistance versus magnetic field for the sample HgSe-M. Traces shown are for **B** lying in a $(1\bar{1}0)$ plane and aligned at various angles to the [110] direction; included are traces for **B** in the [110], [111], and [001] directions. The series of curves in Fig. 7 show how beats in the oscillations build up and then fade as the magnetic-field direction approaches and passes parallelism with the [111] direction; similar behavior occurs when the [001] direction is swept through.

In Table I are listed certain data for a number of samples including those for which curves are shown in Figs. 2–7. The electron concentration in each case was deduced from the Hall coefficient R, by means of the relation $n=1/Rec$. The electron mobilities were computed from $\mu_0=R/\rho_0$. The Hall coefficients were constant for magnetic fields up to 25 kG. No change was observed in R and ρ_0 between 4.2 and 1.2°K. Listed for each sample in Table I is the radius k_F of the spherical surface in **k** space corresponding to the free electron Fermi energy as deduced from the electron concentration:

$$k_F=(2mE_F/\hbar^2)^{1/2}=(3\pi^2n)^{1/3}. \quad (8)$$

TABLE I. HgSe sample characteristics at 4.2°K.

HgSe sample	Electron density $n=1/Rec$ (cm⁻³)	Electron mobility $\mu_0=R/\rho_0$ (cm²/V sec)	Fermi surface radius $k_F=(3\pi^2n)^{1/3}$ (cm⁻¹)
I	1.86×10^{17}	107 000	1.76×10^6
N	2.08×10^{17}	156 000[a]	1.83×10^6
EE	3.47×10^{17}	90 900	2.17×10^6
E	4.46×10^{17}	74 100	2.36×10^6
AA	6.18×10^{17}	65 200	2.63×10^6
K	7.30×10^{17}	56 200	2.78×10^6
M	8.46×10^{17}	49 200	2.92×10^6
L	1.34×10^{18}	80 200[b]	3.40×10^6
CC	2.16×10^{18}	35 900	4.00×10^6
J	4.43×10^{18}	26 700	5.07×10^6
G	4.52×10^{18}	25 700	5.10×10^6

[a] Anomalously large, probably in error. Samples with $n\approx2\times10^{17}$ cm⁻³ usually have $\mu_0\approx110\,000$ cm²/V sec.
[b] Anomalously large, probably in error. Samples with $n\approx1.3\times10^{18}$ cm⁻³ usually have $\mu_0\approx45\,000$ cm²/V sec.

The distance from the origin of **k** space to the nearest point on the first Brillouin zone boundary for HgSe is $\sqrt{3}\pi/2a_0=4.47\times10^7$ cm⁻¹ (a_0, the lattice constant of HgSe, is 6.08 Å). For the samples studied here, the Fermi surfaces had diameters at most only about one-tenth the span of the first Brillouin zone.

Table II lists the periods of the magnetoresistance oscillations for the same samples presented in Table I. The free electron periods were computed from Eq. (4).

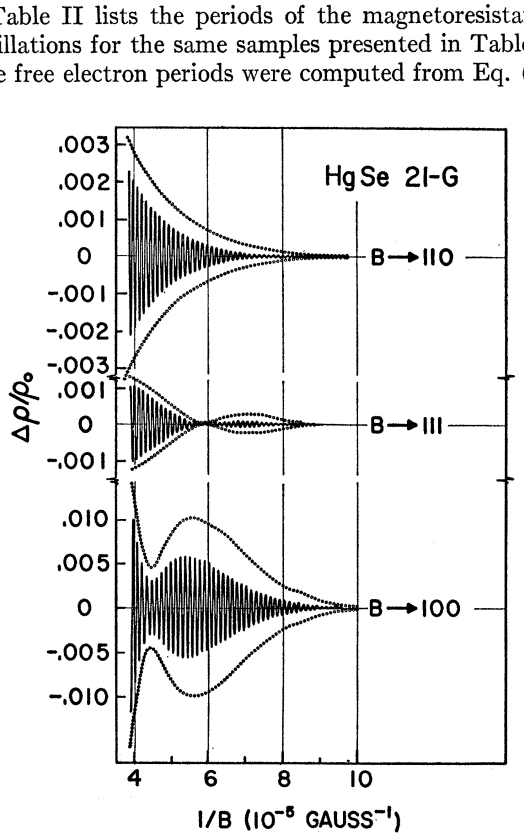

FIG. 6. Oscillatory component of magnetoresistance of HgSe-G; solid curves for 4.2°K, dotted curves for envelopes of oscillations at 1.2°K. At 4.2°K, $n=4.52\times10^{18}$ electrons/cm³ and $\mu_0=25\,700$ cm²/V sec. For no samples was beating observed for B in ⟨110⟩ directions.

TABLE II. Periods of magnetoresistance oscillations in HgSe.

HgSe sample	T (°K)	Calculated free-electron period (10^{-6} G^{-1}) P_F	P_{110}	Measured periods[a] (10^{-6} G^{-1}) (Short period) P^{+}_{111}	(Short period) P^{+}_{100}	(Long period) P^{-}_{111}	(Long period) P^{-}_{100}
I[b]	4.2	9.72	...	...	10.0	...	...
N	4.19	9.01	8.96	9.16	9.19	none	none
	1.19		8.93	9.01	9.14		
EE	4.20	6.42	7.00	7.15	7.41	none	65(6.1,12.6)
	1.18		6.83	7.14	7.34		
E[c]	4.2	5.43	5.47	5.48	5.72	none	none
AA[c]	4.2	4.38	4.26	4.32	4.32	none	none
K[b]	4.20	3.91	...	...	3.99	...	none
	1.19		...	...	3.94		
M	4.18	3.54	3.63	3.65	3.73	>94(66)	>130(130)
	1.18		3.61	3.56	3.68		
L	4.20	2.62	2.58	2.61	2.71	72(57,129)	>70(99)
	1.19		2.54	2.58	2.71		
CC[c]	4.2	1.90	1.84	1.89	1.90	≈45(40)	>30(70)
J[b]	4.20	1.18	...	...	1.21	...	>50(42)
	1.20		...	...	1.20		
G	4.20	1.17	1.26	1.27	1.28	>42(58)	>56(44)
	1.20		1.25	1.26	1.27		

[a] Values for long-beat periods are intervals between first and second nodes of beats; values in parentheses are $1/B$ values of nodes of beats.
[b] Samples not oriented to obtain data for B in ⟨110⟩ and ⟨111⟩ directions.
[c] These samples were not annealed after being cut and had small amplitudes of oscillations which did not change with temperature; beats in oscillations might have been masked by severe damping.

In most cases the free electron periods agree within possible experimental error (±5%) with the measured periods (short periods in the ⟨111⟩ and ⟨100⟩ directions). The ⟨110⟩ periods always are slightly smaller than the ⟨111⟩ and ⟨100⟩ short periods.

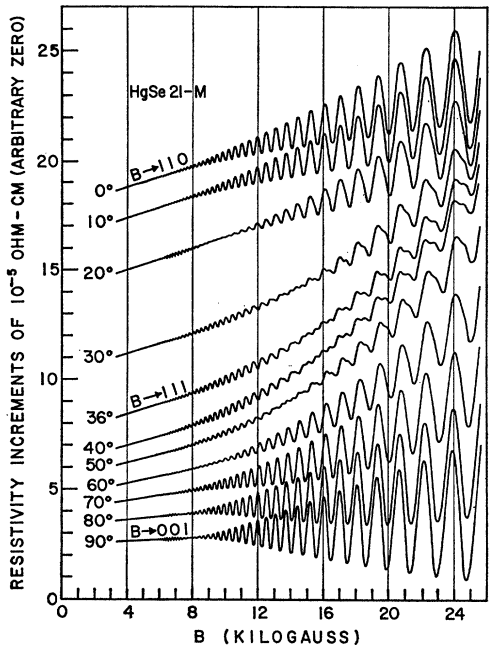

FIG. 7. Resistivity of HgSe-M versus magnetic field for various magnetic-field orientations. Magnetic field was always in (1$\bar{1}$0) plane; angles between magnetic-field direction and [110] direction are given. Zero-field resistivity was 15.0×10^{-5} Ω cm.

Some samples, as noted in Table II, were not annealed after they were cut to size and etched. These samples had magnetoresistance oscillation amplitudes much smaller than those of annealed samples (about one-tenth as large); further, they showed no change in oscillatory amplitude between 1.2 and 4.2°K. It is likely that in the unannealed samples the excess mercury atoms were not homogeneously distributed and that, therefore, the conduction-electron density was not uniform throughout the samples. This would result in a large nonthermal damping of the magnetoresistance oscillations. For some samples, as noted in Table II, there are no ⟨111⟩ and ⟨110⟩ data; these samples were not oriented properly to obtain data for B in the ⟨111⟩ and ⟨110⟩ directions.

Sample HgSe-EE, which had the lowest electron concentration of any for which beating of the oscillations was observed, exhibited a distinct change in periodicity as the magnetic field was varied and other questionable behavior. It may have been that this sample was not homogeneous, and conclusions based upon it are unreliable. The lowest electron concentration for which beating of the oscillations was reliably observed was about 8.5×10^{17} electrons/cm^3.

In every case the oscillatory period at 1.2°K is slightly smaller than that at 4.2°K. The changes are slight enough to be attributable to a systematic error introduced by the method of drawing envelopes in order to obtain the base lines of the oscillations, although examination of the data does not provide grounds for believing this. The shift towards smaller periods at the lower temperature occurs too persistently to be ignored. Such an effect could occur if the lattice contracted and

effected a small net increase in the electron concentration. It also may be that the degree of degeneracy, although high at 4.2°K, increases enough as the temperature is lowered to 1.2°K to produce an observable effect.

THE FERMI SURFACE

For all samples only one period is observed for the magnetic field in a ⟨110⟩ direction, but for all samples with higher electron concentrations the resistance oscillations for the magnetic field in ⟨111⟩ and ⟨100⟩ directions appear to be the superpositions of two oscillatory curves with nearly equal periods. Therefore, the Fermi surface must have only one extremal cross section normal to a ⟨110⟩ direction and must have at least two extremal cross sections normal to a ⟨111⟩ or ⟨100⟩ direction. A very simple model which conforms with these requirements is a deformed sphere that has bulges in the ⟨111⟩ directions. A sketch of this surface, with the bulges exaggerated, is shown in Fig. 8(a). There is a single maximum area normal to the ⟨110⟩ direction enclosed by an orbit as shown in Fig. 8(b). Normal to each of the ⟨100⟩ and ⟨111⟩ directions, as shown in Figs. 8(c) and 8(d), respectively, are a central maximum area and two identical off-center cross sections with relative maximum areas. There must be, of course, cross sections with relative minimum areas between the relative maxima in the ⟨100⟩ and ⟨111⟩ cases.

Let A_{110} be the ⟨110⟩ central cross-sectional area, and let A_0 be the central maximum area and A_{111}, A_{100} the off-center relative maximum areas for the ⟨111⟩, ⟨100⟩ directions. Further, let A_F be the maximum cross-sectional area of a sphere containing the same number of electron states as the deformed sphere ($A_F=\pi k_F^2$). The deformed sphere model for the Fermi surface implies the following resistance oscillation periods:

$$P_{110}(B\rightarrow 110)=(A_F/A_{110})P_F; \quad (9)$$

$$P^{\pm}{}_{111}(B\rightarrow 111)=(2A_F/|A_0\pm A_{111}|)P_F; \quad (10)$$

$$P^{\pm}{}_{100}(B\rightarrow 100)=(2A_F/|A_0\pm A_{100}|)P_F. \quad (11)$$

P_F is given by Eq. (3). There also should be results associated with the relative minimum areas for the ⟨111⟩ and ⟨100⟩ directions. As will be discussed, the bases of the bulges must be quite broad, and therefore the cross sections with minimum areas will be near the origin. The minimum areas in this case will differ only slightly from the central maximum areas and will produce no distinguishable effects.

The observed periods are P_{110}, the short periods $P^{+}{}_{111}$ and $P^{+}{}_{100}$, and the long periods $P^{-}{}_{111}$ and $P^{-}{}_{100}$. Only for sample HgSe-L with B in the ⟨111⟩ direction was a complete long period observed. However, even in this case the magnitude of the long period cannot be stated with confidence because of uncertainty about the relative magnetic-field dependences of the two contributing oscillations. Calculations were made for which it was assumed that the long ⟨111⟩ and ⟨100⟩ periods were either the $1/B$ values at the first long period nodes, or twice these values, in order to get some idea about the various cross-sectional areas of the Fermi surface; results are tabulated in Table III. In spite of the uncertainties in the areas, the results are consistent with the deformed sphere model if the ⟨111⟩ bulge deformities are broad based (perhaps overlapping across {100} planes) and protrude out only about 5% farther than the spherical surface. This model also is consistent with the observed absence of beat oscillations for samples with small electron concentrations if it is assumed that for these the bulges do not protrude far enough for them to give cross-sectional areas which are relative maxima.

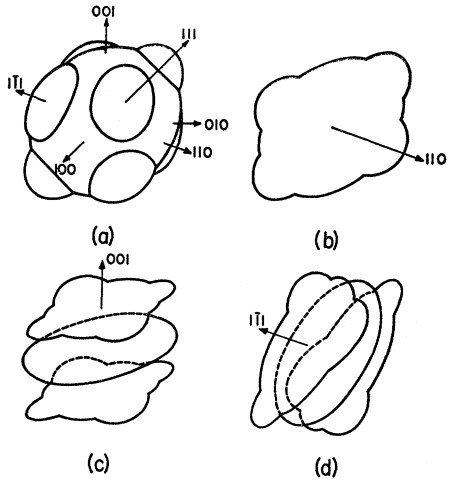

FIG. 8. (a) Fermi-surface model for HgSe. Surface is nearly a sphere with protrusions along ⟨111⟩ directions in **k** space. Protrusions are exaggerated in this drawing. (b) Orbit on Fermi surface enclosing maximum area A_{110} normal to [110] direction. (c) Orbits enclosing relative maximum areas A_0 and A_{100} normal to [001] direction. (d) Orbits enclosing relative maximum areas A_0 and A_{111} normal to [1$\bar{1}$1] direction.

The conclusions in the preceding paragraph are based upon the analysis of a simple mathematical model for the Fermi surface. This model is a sphere with ellipsoidal protrusions in the ⟨111⟩ directions. Such a model can, at best, only approximate the true Fermi surface, but it serves well to verify qualitative features of the true Fermi surface. First, this model always yields $A_{111}>A_{100}$, which is in accord with the analysis of the data. Secondly, in order for the various areas to be as nearly equal as they are indicated to be in Table III, it is necessary for the axes of the ellipsoids aligned with the ⟨111⟩ directions to be very small compared with the perpendicular axes. Thirdly, in order that A_{110} and A_{111} be as nearly equal as they are indicated to be in Table III, and particularly to have A_{110} slightly smaller than A_{111}, it is necessary for the ellipsoidal axes perpendicular to the ⟨111⟩ directions to be large and perhaps even for the ellipsoids to overlap across {100} planes in **k** space. Finally, if the ellipsoids do not protrude far enough there are no off-center extremal cross-sectional areas.

TABLE III. HgSe Fermi-surface extremal cross-sectional (c.s.) areas in units of 10^{12} cm^{-2}.[a]

HgSe sample	Maximum c.s. of free-electron sphere A_F	Maximum c.s. normal to ⟨110⟩ direction A_{110}	Maximum off-center c.s. normal to ⟨111⟩ direction A_{111}	Maximum off-center c.s. normal to ⟨100⟩ direction A_{100}	Maximum central c.s. normal to ⟨111⟩, ⟨100⟩ directions A_0
M	28.2	28.5	28.9–29.9	26.8–28.0	26.6–27.6
L	38.2	39.4	39.7–40.6	36.4–37.9	35.9–37.9
CC	52.6	54.4	54.0–55.1	53.1–53.6	50.7–52.1
J	84.8	···	···	83.8–85.0	80.1–81.3
G	85.5	80.0	80.3–81.1	79.8–81.0	76.4–78.6

[a] Lower limits given in each case are based upon the assumption that the long-beat period is 2× (1/B value at first node of beat); upper limits based upon the long period being 1/B value at first node of beat. Two c.s. areas are calculated for both ⟨111⟩ and ⟨100⟩ directions; the most nearly equal ⟨111⟩ and ⟨100⟩ areas are assumed to be A_0.

Because of the ⟨111⟩ protrusions the bottom of the conduction band must be lowest for **k** in a ⟨111⟩ direction as is indicated in Fig. 1.

THE EFFECTIVE MASS

At a given magnetic field the variation with temperature of the oscillation amplitudes is given entirely by the term $\xi/\sinh\xi$ in Eq. (5). Because of the near sphericity of the Fermi surface it will be assumed that the cyclotron frequency is $\omega=eB/cm^*m_e$, where m^* is the ratio at the Fermi surface of the cyclotron effective mass [defined in Eq. (6)] to the free electron mass. If the oscillatory amplitude at a given magnetic field is a_1 at a temperature T_1, and is a_2 at a temperature T_2, then by Eq. (5),

$$\frac{a_1}{a_2}=\frac{T_1\sinh(2\pi^2kT_2cm^*m_e/heB)}{T_2\sinh(2\pi^2kT_1cm^*m_e/heB)}. \qquad (12)$$

This was solved for m^* at several values of magnetic field for each sample.

Figure 9 shows the m^* values determined in this manner at several values of 1/B for each of the annealed samples. For HgSe-G, with B in a ⟨110⟩ direction, the value of m^* varies widely for different fields, and obviously Eq. (5) does not give the correct temperature dependence of the oscillation amplitudes for this sample. However, for the other samples, the calculated m^* values are fairly constant over a wide range of magnetic fields.

The averages of the mass ratios calculated for each sample and for each direction of magnetic field are listed in Table IV. The amount of scatter of m^* values calculated from what were judged to be reliable amplitude measurements was ±0.001 or less except where otherwise indicated in Table IV.

The variation of effective mass with electron concentration is shown in Fig. 10; also shown are the cyclotron effective-mass ratios at room temperature as deduced by Wright, Strauss, and Harman[11] from reflectivity data. The agreement between the two sets of results, determined by totally unrelated methods, is strikingly good.

TABLE IV. HgSe cyclotron-effective-mass ratios.[a]

HgSe sample	Calculated m^* (Kane band model)	m^* for B in ⟨110⟩ direction	m^* for B in ⟨111⟩ direction	m^* for B in ⟨100⟩ direction
I	0.035	···	···	0.033
N	0.035	0.035	0.034	0.031
EE	0.038	0.036±0.003	0.037±0.002	0.037±0.002
K	0.044	···	···	0.042
M	0.045	0.044	0.044	0.041
L	0.050	0.048	0.048±0.002	0.048±0.002
J	0.067	···	···	0.065±0.002
G	0.068	0.068±0.006	0.065±0.010	0.063±0.003

[a] The ratio m^* is m_H/m_e where m_H is the cyclotron mass and m_e is the free-electron mass. Values listed are averages of those computed for several magnetic-field strengths; scatter of points was ±0.001 or less except where otherwise indicated.

From these cyclotron effective-mass data some of the conduction-band parameters for HgSe may be deduced.

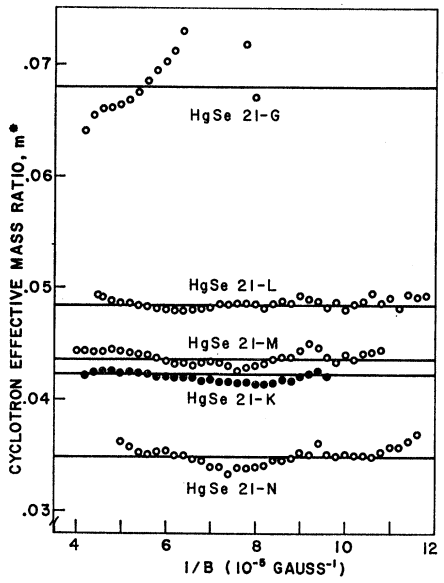

FIG. 9. Cyclotron-effective-mass ratios for various 1/B values as deduced from the temperature dependence of magnetoresistance oscillation amplitudes. Points are from curves for B in a ⟨110⟩ direction except for HgSe-K for which B was in a ⟨100⟩ direction.

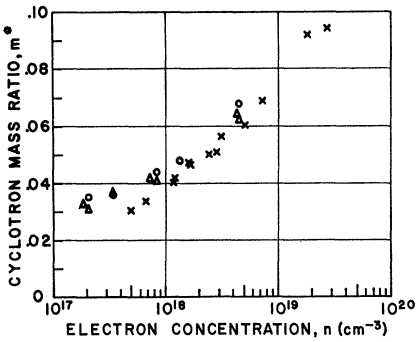

FIG. 10. Cyclotron-effective-mass ratio m^* versus conduction-electron concentration n: ○ for B in ⟨110⟩ direction, Δ for B in ⟨100⟩ direction, × for points deduced from optical-reflectivity data in Ref. 11.

On the basis of the calculations by Kane[14] for InSb, the conduction-band energy, measured from the bottom of the conduction band, is given by

$$E_C=\hbar^2k^2/2m_e-E_G/2+\tfrac{1}{2}(E_G^2+8P^2k^2/3)^{1/2}, \quad (13)$$

where E_G is the forbidden energy gap at $\mathbf{k}=0$ and P is an interband momentum matrix element defined by Kane. Equation (13) is an approximation which should be valid if the spin-orbit splitting Δ of the valence bands is much larger than E_G. Since for HgSe, the spin-orbit splitting should be ≈ 1 eV and E_G is only 0.2 eV, Eq. (13) should be expected to hold. The cyclotron effective mass ratio is then, from Eqs. (6) and (13),

$$m^*=m_H/m_e=\left[1+\frac{4m_eP^2}{3\hbar^2}(E_G^2+8k^2P^{2/3})^{-1/2}\right]^{-1}. \quad (14)$$

If the relation $k=(3\pi^2n)^{1/3}$ is used, Eq. (14) will yield

$$[m^*/(1-m^*)]^2=32.5\times10^{-32}(E_G^2/P^4)+8.29\times10^{-30}(n^{2/3}/P^2), \quad (15)$$

where the numerical factors are those appropriate if the units for E_G, P, and n are eV, eV cm, and cm^{-3}, respectively. Thus, a plot of $[m^*/(1-m^*)]^2$ versus $n^{2/3}$ should give a straight line with slope proportional to $1/P^2$ and with an intercept proportional to E_G^2/P^4. An analysis of such a plot based upon what were judged to be the most accurate m^* values of this study gave $P=7.1\times10^{-8}$ eV cm and $E_G=0.24$ eV; a plot including all of the obtained m^* values gave $P=(7.4\pm0.4)\times10^{-8}$ eV cm and $E_G=0.25\pm0.05$ eV. Wright, Strauss, and Harman[11] from their data deduced $P=8\times10^{-8}$ eV cm and $E_G=0.2$ eV. In the present study, the masses determined for samples with carrier concentrations less than 10^{18} cm^{-3} were the more reliable, whereas the masses deduced from reflectivity measurements were more accurate for higher electron concentrations. In both cases, the effective-mass variation with electron concentration is in accord with the Kane conduction-band model, and the value found for P (7–8×10^{-8} eV cm) compares with the value 8.7×10^{-8} eV cm found for InSb[21] which has about the same energy gap as HgSe at $\mathbf{k}=0$.

The values $P=7.1\times10^{-8}$ eV cm and $E_G=0.24$ eV give values for E_F ranging from 0.041 to 0.22 eV and values for $\hbar\omega$ at 10 kG ranging from 0.0033 to 0.0017 eV as n is increased from 2×10^{17} to 5×10^{18} electrons/cm^3. At the lowest concentration reported upon here, 2×10^{17} electrons/cm^3, E_F is about equal to $13\hbar\omega$ at 10 kG. At 1.2 and 4.2°K, kT has the values 1.0×10^{-4} and 3.6×10^{-4} eV, respectively; thus, at 10 kG, even for the highest electron concentration, $\hbar\omega$ is much greater than kT. The energy requirements for observation of oscillatory phenomena therefore are met.

The degeneracy of the samples that have the lowest electron concentrations is weak enough that the change in Fermi energy between 1.2 and 4.2°K is significant. For $n=2\times10^{17}$ electrons/cm^3, the Fermi energy decreases by 0.06% as T increases from 1.2 to 4.2°K. This is not as large a percentage change as the observed changes in periods between 1.2 and 4.2°K, but it does contribute in the right way to help explain the period shifts.

NONTHERMAL DAMPING

The damping of the oscillations for the magnetic field in the ⟨111⟩ and ⟨100⟩ directions was not analyzed because of the beat patterns. Since the amplitudes decreased smoothly as $1/B$ increased when the field was in the ⟨110⟩ direction, these could be analyzed. For each sample and for several values of magnetic field, the nonthermal damping factor γ in Eq. (5) was calculated. For these calculations, the measured periods were substituted for $\hbar\omega/E_F$, the envelopes of the oscillations

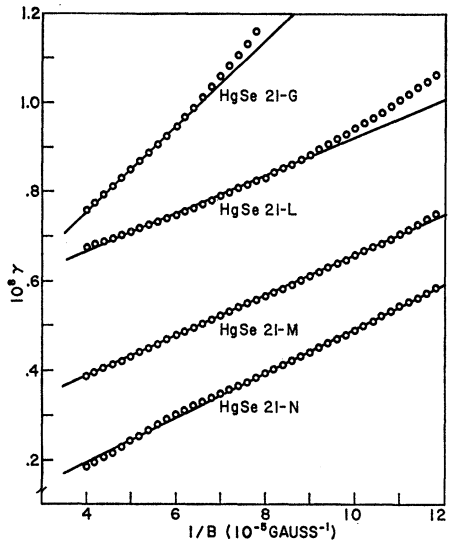

FIG. 11. Nonthermal damping factor γ versus $1/B$ for HgSe samples. Slopes of plots were used to deduce effective collision times τ_c, mobilities μ_c, and temperatures T' listed in Table V.

[21] G. B. Wright and B. Lax, J. Appl. Phys. 32, 2113 (1961).

were used to determine $\Delta\sigma/\sigma_0$, and the average value of m_H, determined in the preceding section, was used to replace $\hbar\omega$ by $\hbar eB/cm_H$ in the thermal damping term. Figure 11 shows plots of γ versus $1/B$ determined in this manner. Practically identical plots were obtained for both 1.2 and 4.2°K except for sample HgSe-G at higher $1/B$ values. Some of the plots are linear, and that for sample HgSe-N extrapolates to close to the origin. Except for HgSe-G, the plots have approximately the same slopes but are displaced upwards for increasing electron concentrations.

The nonthermal damping factor γ is determined both by the probability for scattering of electrons (particularly at those values of magnetic field for which a Landau cylinder just emerges from the Fermi surface) and by the inhomogeneity of the sample. If Eq. (5) does give the correct magnetic field dependence of $\Delta\sigma/\sigma_0$, then the slopes of the plots in Fig. 11 can be used to derive effective values for a collision time τ_c, a mobility μ_c, or a temperature T' defined by:

$$\tau_c=(e/cm_H)d\gamma/d(1/B); \tag{16}$$

$$\mu_c=e\tau_c/cm_H; \tag{17}$$

$$T'=\hbar/\pi k\tau_c. \tag{18}$$

The effective values so defined and as determined from the slopes drawn in Fig. 11 are given in Table V. These

TABLE V. Nonthermal damping parameters for magnetoresistance oscillations in HgSe.

HgSe sample	Collision time $\tau_c=(e/cm_H)\times d\gamma/d(1/B)$ (sec)	Effective mobility $\mu_c=e\tau_c/cm_H$ (cm²/V sec)	Effective temperature $T'=\hbar/\pi k\tau_c$ (°K)
N	3.8×10^{-13}	20 000	6.1
M	5.4×10^{-13}	21 900	5.5
L	1.2×10^{-12}	23 300	3.9
G	4.0×10^{-13}	10 300	6.4

parameters are chiefly an indication of the quality of the samples. A quantitative theory of the resultant effect of combined collision and inhomogeneity damping might enable more information, particularly about the magnetic-field dependence of collision broadening, to be extracted from the data.

The failure of the plots in Fig. 11 to extrapolate to the origin implies the existence of a damping term independent of magnetic field and temperature. Such a term might derive from an implicit magnetic-field dependence of τ_c or from the nature of inhomogeneity broadening. In any event, this damping is more severe as the electron concentration, and hence the excess of mercury, is increased in HgSe.

DISCUSSION

To accurately determine the contours of the Fermi surface in HgSe, highly precise measurements extending to higher magnetic fields are needed as well as measurements for other directions of magnetic field in addition to those of this study. High precision is required because small errors in any of the oscillatory period determinations lead to gross uncertainties about the sizes of the protrusions from the Fermi surface. Determinations for a number of magnetic field orientations will enable the shapes of the protrusions to be deduced. More details of the interference of the beating oscillatory components (such as their relative magnitudes and phase separations) should be discernable at higher magnetic fields.

For the samples with very small electron concentrations ($<5\times10^{17}$ electrons/cm³) the Fermi energy lies below the top of the overlapping valence band if the overlap energy of 0.07 eV deduced by Harman and Strauss[2] is correct. In these samples, there should be significant concentrations of holes, but the influence upon transport effects by the holes can be only very slight because of the large effective hole mass. Contributions by holes to the oscillatory magnetoresistance would be damped out at all but very high magnetic fields. Further, it is likely that the overlapping valence band is a many-valley band and the hole Fermi surface will be a family of small ellipsoids. The cross sections of these hole surfaces will be small and the oscillatory periods due to holes will be larger than those due to electrons. Therefore, there will be few hole oscillations at the high magnetic fields where they might be distinguished from oscillations due to electrons. It appears that it will be extremely difficult to observe oscillations due to holes unless, of course, the electron concentration can be reduced much below those reported here in order that the slight hole effects will not be masked. An effort to obtain direct evidence for the existence of holes and the overlapping valence band is nevertheless to be desired, because positive results would not only confirm the prediction of Harman and Strauss, but would allow band parameters to be determined for the valence band and would justify more detailed theoretical work on the valence band structures in zincblende compounds.

It also would be particularly interesting to extend studies of the oscillatory magnetoresistance in HgSe to samples with higher electron concentrations than those reported upon here. These studies should employ much higher magnetic fields in order to observe complete beat periods and to obtain more detailed information about the interfering oscillatory components. At sufficiently large electron concentrations there may be a many-valley electron Fermi surface in HgSe. If corrections due to higher lying energy bands are used, the conduction band may not have its maximum energy at a Brillouin zone boundary (see Cardona[16]). If the maximum is not at the zone boundary, then, for sufficiently high electron concentrations, there will be pockets of occupied electron states on certain of the Brillouin zone faces. To be expected for sufficiently large electron concentrations, therefore, are small-period oscillations due still to the deformed sphere centered at the origin of $\mathbf{k}$ space and

other, longer period, oscillations due to pockets of the Fermi surface on the Brillouin zone boundaries.

CONCLUSIONS

From the nature of the variation of the oscillatory magnetoresistance with orientation of the magnetic field it is concluded that the Fermi surface for HgSe has protrusions in the ⟨111⟩ directions of k space. These protrusions, however, are small in height and the Fermi surface is not much deformed from a spherical shape. The existing theories adequately describe the temperature dependence of the amplitudes of the magnetoresistance oscillations in HgSe, and this temperature dependence yields values for the cyclotron effective masses of conduction electrons in good agreement with those deduced from optical reflectivity data. The variation of effective mass with conduction electron density is in accord with energy band models proposed for materials that have the zincblende structure, and this variation of effective mass was used to determine the energy gap at $\mathbf{k}=0$ and the curvature of the conduction band in HgSe.

ACKNOWLEDGMENTS

Ralph D. Thomas prepared the crystals for this investigation and performed much of the data collection and reduction. His assistance was invaluable and is gratefully acknowledged. Thanks are given to David E. Soule, who was the first to observe magnetoresistance oscillations in HgSe, for the use of his magnet and cryogenic facilities for this work. Discussions with Joel W. McClure and Glen C. Wagoner during the course of this work were very helpful. Thanks also are given to Robert P. Ulman, who assisted in obtaining some of the data, and to Carl Lowell who did the x-ray diffraction work necessary for crystallographically orienting the crystals.

PHYSICAL REVIEW VOLUME 138, NUMBER 3A 3 MAY 1965

Optical Probing of the Environment of F Centers in Deformed Alkali Halides*

R. CHANG
North American Aviation Science Center, Thousand Oaks, California
(Received 7 December 1964)

The formation of F centers upon Co^{60} irradiation of KCl deformed at room temperature and at 77°K and the environment of F centers formed upon Co^{60} irradiation of deformed KBr were studied by means of optical-absorption measurements with a Cary-14 spectrophotometer. Anomalies of the beta absorption band (exciton band localized at the F centers) and shift of the F-center peak toward blue were observed in deformed KBr at 10 and 80°K. The observed anomalies can be removed by a short annealing near 525°K. Both the dichroic behavior of the beta band and the energy shift of the F band are consistent with the hypothesis that the source of vacancies is the edge-dislocation dipoles from plastic deformation. The F centers formed upon Co^{60} irradiation of deformed KBr are most probably located a few Burgers vectors away from the core of one member of the edge-dislocation dipole in the compression region, a fraction of an interatomic spacing above the slip plane where the edge dislocation is situated.

I. INTRODUCTION

A QUALITATIVE interpretation of the various effects of mechanical deformation on coloration phenomena has been proposed by Seitz,[1] who suggested that mechanical deformation results in an increase in the vacancy concentration. The increased darkenability of deformed crystals and the bleaching effect of plastic deformation of a crystal previously colored by irradiation are understandable in a general sense according to this hypothesis. On the other hand, Nowick[2] ascribes the enhancement of the colorability of the annealed crystals upon plastic deformation to the dispersing action of the plastic deformation, which causes the precipitated impurities to be redissolved on an atomic scale. Smoluchowski and co-workers[3,4] have made extensive studies of the growth of the F band in undeformed, deformed, and heat-treated KCl crystals between liquid-hydrogen temperature and room temperature. The similarity in forms and temperature dependence of the initial coloration in a freshly cleaved crystal and the coloration after plastic deformation suggests that both these stages obtain vacancies from the same source, and they concluded that the source of vacancies is the debris resulting from dislocation interaction and not from the dislocation lines themselves. Further experimental evidence of enhanced coloration in deformed KCl due to the presence of dislocation dipoles is seen in the work of Davidge and Pratt,[5] who remarked,

* This work was supported in part by the U. S. Office of Naval Research (Contract NONR-4063-00, NR-032-479), Department of the Navy.
[1] F. Seitz, Phys. Rev. **80**, 239 (1950).
[2] A. S. Nowick, Phys. Rev. **111**, 16 (1958).
[3] P. V. Mitchell, D. A. Wiegand, and R. Smoluchowski, Phys. Rev. **121**, 484 (1961).
[4] B. S. H. Royce and R. Smoluchowski, Discussions Faraday Soc. (to be published).
[5] R. W. Davidge and P. L. Pratt, Phys. Stat. Solidi **3**, 665 (1963).